Flexible high-frequency microwave inductors and capacitors integrated on a polyethylene terephthalate substrate

Lei Sun,[1] Guoxuan Qin,[1] Hai Huang,[1] Han Zhou,[1] Nader Behdad,[1] Weidong Zhou,[2] and Zhenqiang Ma[1,a)]
[1]*Department of Electrical and Computer Engineering, University of Wisconsin-Madison, Madison, Wisconsin 53706, USA*
[2]*Department of Electrical Engineering, University of Texas-Arlington, Arlington, Texas 76019, USA*

(Received 7 September 2009; accepted 4 December 2009; published online 6 January 2010)

This letter reports the realization of bendable inductors and capacitors integrated on a polyethylene terephthalate substrate that can operate at high microwave frequencies. A low-temperature fabrication process compatible with flexible thin-film transistors (TFTs) was developed. By employing bendable dielectric materials, spiral inductors and metal-insulator-metal capacitors with high quality factors and high resonance frequencies were demonstrated. The effects of mechanical bending on the performance of inductors and capacitors were also measured and analyzed. These demonstrations combined with previously demonstrated microwave TFTs will lead to flexible radio-frequency and microwave systems in the future. © *2010 American Institute of Physics*. [doi:10.1063/1.3280040]

Flexible electronics, because they are light weight, robust, easy to bend and fold, and mountable to uneven surfaces, have been investigated intensively in recent years.[1,2] Presently, flexible electronics were implemented mainly in low-speed applications, such as flexible displays,[3,4] electronic tags,[5,6] etc. The cause of this circumstance is the lack of high-speed active semiconductor materials that can be used for flexible electronics. Currently, the commonly used amorphous silicon, organic polymers, and polycrystalline semiconductor materials can only provide low-speed active devices. Regardless, there has been a long desire for high-speed (beyond 1 GHz operation frequency) flexible electronics. With high speed, flexible electronics would find a wider range of applications than their low-speed counterparts. While dramatic power consumption can be saved when using high-speed devices at reduced low speed, high-speed flexible electronics are exceptionally wireless capable. Thus they can be used for personal Wi-Fi devices, wearable radios, radio-frequency (rf) identification devices, foldable phased-array antennas, large-area radars for remote sensing, surveillance,[7] etc. Nonetheless, current high-speed devices have been predominantly made of rigid chips and none of the traditional flexible active semiconductors can fulfill the requirements of any high-speed applications.

Lucratively, the technical barriers of using flexible electronics for high-speed applications have recently been broken by the introduction of high-mobility transferable single-crystal semiconductor membranes,[8] the development of effective processing techniques for these materials,[9] and the advanced active device structures.[10] The current high speed of flexible thin-film transistors (TFTs) (Ref. 10) realized with the transferable membranes has demonstrated the potential of using these types of devices for high-frequency microwave operations.

To implement these high-speed microwave flexible TFTs in functional circuits and systems, high-frequency microwave passive components, such as inductors, capacitors, and transmission lines, are needed. Of more critical importance, the passives also need to be mechanically flexible, robust, and can be integrated together with the high-speed TFTs on the same low-temperature substrates. Although some bendable discrete inductors and capacitors were already made on polyimide substrate, they worked in the relatively low-frequency range and cannot be monolithically integrated with flexible active TFTs.[11–13] In this letter, we report the fabrication and characterization of flexible high-frequency inductors and capacitors monolithically integrated on a polyethylene terephthalate (PET) substrate. By using the fabrication process compatible with that of the recent microwave TFTs, high performance inductors and capacitors with excellent bendability are shown to be achievable.

The process began with optical photolithography on a PET substrate (5 mil). A 30/400 nm Ti/Au metal was deposited on the PET substrate by electron-beam (e-beam) evaporation followed by a liftoff [Fig. 1(a)]. This metal layer (M1) serves as the bottom electrode of metal-insulator-metal (MIM) capacitors and the center lead metal of spiral inductors.

In conventional rigid chip based integrated circuit technology, on-chip MIM capacitors are conveniently implemented between interconnect metal layers with plasma-enhanced chemical vapor deposited (PECVD) dielectrics. The typical PECVD deposition temperature is about 300–350 °C. Such a temperature is not suitable for PET substrates because the Vicat softening temperature of PET is only 170 °C. In order to form the MIM capacitors, a silicon monoxide (SiO) (ε_r=5.8–10, depending on stoichiometry) layer with 200 nm thickness was e-beam evaporated in vacuum on the top of the bottom electrode of the capacitors at room temperature. Following the SiO deposition, another metal layer (M2) consisting of Ti/Au metal (30/400 nm) was then evaporated on the top of the patterned SiO dielectric layer as the top electrode to form the MIM structure of the capacitors [Fig. 1(b)]. The SiO and the M2 layers were then lifted off together.

a)Author to whom corresponding should be addressed: Electronic mail: mazq@engr.wisc.edu.

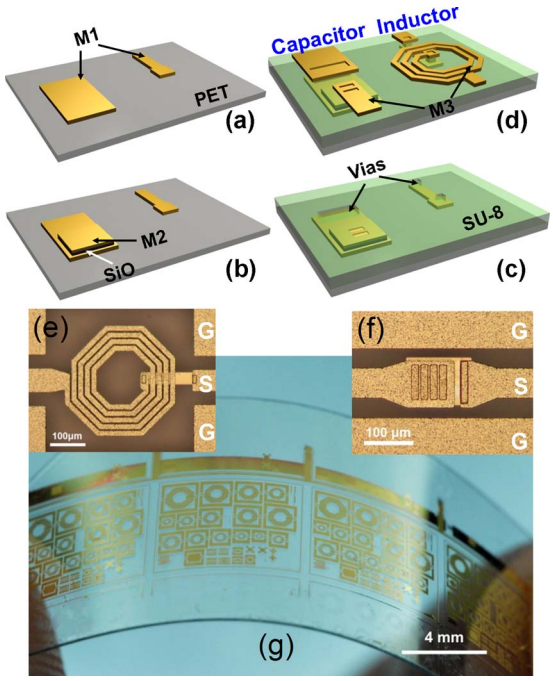

FIG. 1. (Color online) Illustration of fabrication process for integrated flexible spiral inductors and MIM capacitors. (a) M1 was evaporated on a PET substrate to form the bottom electrode of MIM capacitors and the center lead metal of inductors. (b) A 200 nm SiO layer was evaporated on top of bottom electrode as the capacitor high-k dielectric. M2 was evaporated on top of SiO to form the top electrode for capacitors. The two layers were lifted together to form a self-aligned structure. (c) A layer of 1.0 μm SU-8 was spun on to act as intermetal low-k isolation layer. Via holes were opened with lithography and SU-8 was cured to cross link. (d) M3 was evaporated to form the spiral metals of inductors and interconnects. An optical-microscope image of (e) a 4.5-turn spiral inductor, (f) a 88 $\times$88 μm^2 MIM capacitor, and (g) finished inductor and capacitor arrays on a bent PET substrate.

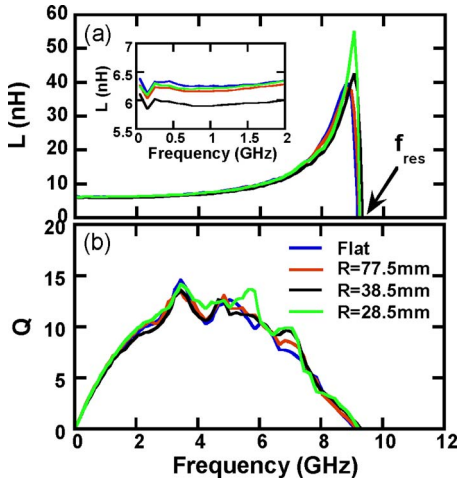

FIG. 2. (Color online) Measured (a) L values and (b) Q values of a 4.5-turn spiral inductor as a function of frequency under flat and bending conditions. The spiral metal line width is 15 μm and the metal line spacing is 4 μm. The inset of (a) shows the zoom in of L values in the low frequency range. The f_{res} is indicated by the zero L and zero Q values. The two figures have the same X-axis scale.

For the MIM capacitors, a higher dielectric constant (high-k) and a smaller thickness are desired for high-density capacitors and thus reduced capacitor size. However, this requirement is contradictory to that for spiral inductors. A smaller intermetal dielectric constant (low-k) will result in a smaller parasitic capacitance and thus higher resonance/operation frequencies for inductors. To solve this dilemma, we used relatively thick ($\sim$1 μm) SU-8 (MicroChem) (dielectric constant ε_r=3) as the intermetal dielectric (also very flexible) for the spiral inductors. The SU-8 was spun on the sample surface followed by a photolithography patterning step to open up via holes in order to access the bottom and the top electrodes of the capacitors and the center lead metal of the inductors. SU-8 was then cured to cross link for 45 s under UV exposure and a 115 °C hard baking [Fig. 1(c)]. Finally, a 30 nm/1.5 μm Ti/Au top interconnect metal (M3) was evaporated to form the spiral metal of the inductors and to make interconnects (e.g., ground-signal-ground) for both the inductors and the capacitors [Fig. 1(d)]. The use of thick metal for M3 was to reduce the parasitic resistance of the devices (particularly for multiple turn inductors) in order to realize high-frequency operations. The use of the octagonal shape for the inductors was intended to reduce the sharp-bending microwave loss at high frequencies.

Overall, three metal layers and two dielectric layers were used to form the integrated passive components on a single PET substrate. The thin (maximum thickness: $\sim$3.5 μm) and planar structures of the devices make them highly robust to mechanical bending and are also suitable for achieving high-frequency operations. The thermal budget of the entire process was under 120 °C (photoresist baking temperature), which can easily satisfy the tolerance of most low-temperature plastic substrates. Of more significance, the fabrication process is completely compatible with that used to fabricate microwave TFTs.[9,10] Figures 1(e) and 1(f) show optical images of a 4.5-turn inductor and a 7744 μm^2 MIM capacitor on a PET substrate, respectively. The spiral metal lines of the inductors have a width of 15 μm and a spacing of 4 μm. Figure 1(g) shows inductor and capacitor arrays on a bent PET substrate.

The rf characteristics of the fabricated inductors and capacitors were measured with an Agilent E8364A performance network analyzer (45 MHz–40 GHz) and an Agilent 5230A (300 kHz–20 GHz) network analyzer. The critical passive component parameters, such as inductance/capacitance (L/C) values, quality factor (Q) values, and resonant frequency values, were extracted from measured scattering (S) parameters.

The measured L and Q values of a 4.5-turn inductor as a function of frequency are plotted in Figs. 2(a) and 2(b), respectively. A constant L value of $\sim$6 nH was measured from 45 MHz up to $\sim$5 GHz, with an f_{res} of 9.1 GHz. The peak Q of 14.6 was measured at 3.45 GHz [see Fig. 2(b)]. Such a high Q and a high f_{res} make the spiral inductors implementable for rf circuits up to $\sim$8 GHz, sufficiently meeting the active TFT operation frequency requirement.[10] Figure 2 also shows the results of bending test (along the input-output direction) for the spiral inductors. In general, as the convex bending radius was reduced, the L values at low frequency slightly decrease, while a slight increase of both peak Q and f_{res} was observed [also see Fig. 4(a)]. These results indicate that the spiral inductors fabricated on the plastic substrate exhibit very good mechanical robustness.

MIM capacitors with different periphery-to-area (P/A) ratios were also measured. The measured C values versus frequency for a 40$\times$40 μm^2 capacitor under both flat and different bending states are shown in Fig. 3. A value of 0.45 pF at 4 GHz was measured with a f_{res} of 13.5 GHz, even

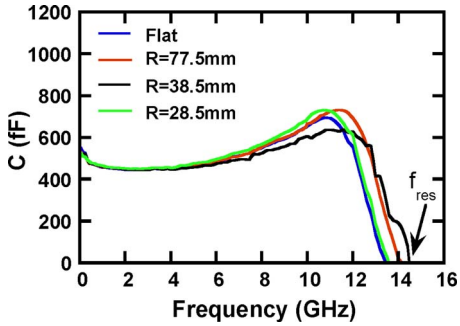

FIG. 3. (Color online) Measured capacitance values of a 40×40 μm^2 MIM capacitor as a function of frequency under flat and bending states. The f_{res} is indicated by the zero capacitance values.

though the associated interconnect parasitics were not de-embedded. The Q value is measured to be 6.4 at 4 GHz. In general, both the values of C and f_{res} were slightly increased as the convex bending radius is decreased [see Fig. 4(b)].

To understand the bending effects on the rf characteristics of the inductors and capacitors (see Fig. 4), we simulated the two devices under bending conditions with CST MICROWAVE STUDIO® (software made by Computer Simulation Technology). When the inductor was bent, although the shape of the inductor was slightly distorted due to substrate induced strain, the total magnetic field remains almost unchanged. However, the perpendicular (relative to inductor surface) component of the magnetic flux through the hollow center of the inductor, which determines the inductance values, was reduced under bending. The reduced inductance also results in slight increase of f_{res} (parasitic capacitance

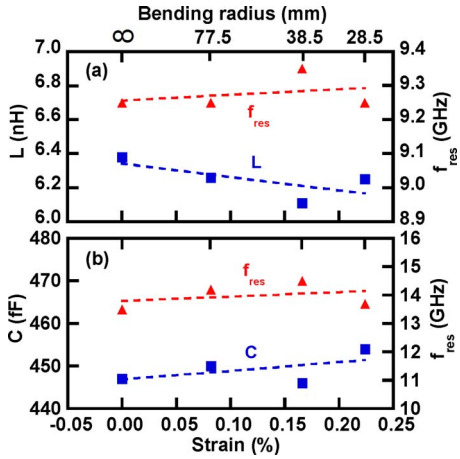

FIG. 4. (Color online) (a) Measured L (values take at 45 MHz) and f_{res} of a 4.5-turn spiral inductor, and (b) measured C (values take at 4 GHz) and f_{res} of a 40×40 μm^2 MIM capacitor under different bending radii. The values of tensile strain were calculated from the bending radii. The dashed lines are fitted trend lines for the measured data points.

was not affected by bending). Since the inductor surface area is relative small in comparison to even the smallest bending radius, the overall effect of bending on the inductor performance is not magnificent.

When the capacitor was bent, the area of the capacitor was increased (Poisson's effect on PET was included) and the capacitor dielectric thickness may also be reduced. The capacitance values were thus increased. In the mean time, the vertical vias of the capacitors [Fig. 1(c)] were also distorted and stretched, with reduced parasitic inductance values. The measured increase of f_{res} with the decrease of bending radius [Fig. 4(b)] indicates that the parasitic inductance change is the dominant reason for the change.

In summary, employing a fabrication process compatible with microwave TFTs, high-frequency microwave flexible inductors and capacitors have been demonstrated on low-temperature plastic substrates. Both high Q and high f_{res} were achieved from the passive devices. Robust mechanical characteristics were also exhibited by these high-frequency passives. Collectively, these passives can fulfill the frequency requirements of flexible rf circuits up to 8 GHz. Further integration of these passive components with high speed flexible TFTs will eventually lead to flexible rf systems.

This work was supported by AFOSR MURI project under Grant No. FA9550-08-1-0337. The program manager is Dr. Gernot Pomrenke.

[1]S. R. Forrest, Nature (London) **428**, 911 (2004).
[2]Y. Sun and J. A. Rogers, Adv. Mater. **19**, 1897 (2007).
[3]Y. Chen, J. Au, P. Kazlas, A. Ritenour, H. Gate, and M. McCreary, Nature (London) **423**, 136 (2003).
[4]G. H. Gelinck, H. E. A. Huitema, E. van Veenendaal, E. Cantatore, L. Schrijnemakers, J. B. P. H. Van der Putten, T. C. T. Geuns, M. Beenhakkers, J. B. Giesbers, B.-H. Huisman, E. J. Meijer, E. M. Benito, F. J. Touwslager, A. W. Marsman, B. J. E. van Rens, and D. M. de Leeuw, Nature Mater. **3**, 106 (2004).
[5]P. F. Baude, D. A. Ender, M. A. Haase, T. W. Kelley, D. V. Muyres, and S. D. Theiss, Appl. Phys. Lett. **82**, 3964 (2003).
[6]V. Subramanian, P. C. Chang, J. B. Lee, S. E. Molesa, and S. K. Volkman, IEEE Trans. Compon. Packag. Technol. **28**, 742 (2005).
[7]R. H. Reuss, B. R. Chalamala, A. Moussessian, M. G. Kane, A. Kumar, D. C. Zhang, J. A. Rogers, M. Hatalis, D. Temple, G. Moddel, B. J. Eliasson, M. J. Estes, J. Kunze, E. S. Handy, E. S. Harmon, D. B. Salzman, J. M. Woodall, M. A. Alam, J. Y. Murthy, S. C. Jacobsen, M. Oliver, D. Markus, P. M. Campbell, and E. Snow, Proc. IEEE **93**, 1239 (2005).
[8]E. Menard, K. J. Lee, D.-Y. Khang, R. G. Nuzzo, and J. A. Rogers, Appl. Phys. Lett. **84**, 5398 (2004).
[9]H.-C. Yuan and Z. Ma, Appl. Phys. Lett. **89**, 212105 (2006).
[10]H.-C. Yuan, G. K. Celler, and Z. Ma, J. Appl. Phys. **102**, 034501 (2007).
[11]T. Lenihan, L. Schaper, Y. Shi, G. Morcan, and J. Parkerson, Electronic Components and Technology Conference, 1996 (unpublished), p. 119.
[12]E. Waffenschmidt, B. Ackermann, and M. Wille, Power Electronics Specialists Conference, 2005 (unpublished), p. 1528.
[13]H. C. Lim, J. Zunino, and J. F. Federici, Sens. Transducers J. **91**, 39 (2008).